Experimental Identification of Modal Density Parameters of Light Weight Structures

A.M. Fareed, G. Schmidt, F. Wahl

A basic requirement for the analysis of vibro-acoustic problems by means of the Statistical Energy Analysis (SEA) is the knowledge of modal densities of the tested subsystems. For simple structures, modal densities are obtained by theoretical solutions. The application of the SEA to complex light weight structures often leads to sophisticated subsystems the modal densities of which cannot be received from theoretical solutions. Therefore, experimental procedures for the identification of modal densities are needed. This paper describes an experimental method based on the theoretical relation between the modal density and the real part of the point admittance, the conductance. Simulations of a simply supported rectangular plate show the accuracy and the limits of the method. A steel plate and a thin-walled cylinder made of fiber composite material have been thoroughly investigated by experiments. By this, the influence of the mass correction of the measured conductances is discussed in the paper. The experimental results are compared with theoretical results obtained from the code AutoSEA2. For medium and higher frequencies the results are in fairly good agreement.

1 Introduction

The statistical energy analysis (SEA) method is increasingly used to describe the vibro-acoustic behaviour of complex structures. This method is used for example to determine the sound power in space structures, to calculate the energy transfer through the substructures, to determine the internal and coupling loss factors of substructures, etc.. This method is proposed in general for medium and high frequency vibration and noise prediction. The statistical nature of SEA allows for a structure with many resonances to be modelled in a deterministic model. The SEA model is based on a balance of the dynamical energy and power flows among groups of natural modes in a structure. A complex structure is modelled as a set of coupled mode groups or substructures (Lyon and DeJong, 1995). The modal densities of these substructures are then approximated by mathematical expressions for simple structures. These expressions can be incorrect, since boundary conditions are neglected (Serati and Marshall, 1989). The successful application of SEA depends strongly upon the high modal density and the high modal overlap of the structure under investigation to ensure good average modal densities.

This paper aims to explain the use of an experimental procedure to measure the conductance, the real part of the admittance, and to calculate the modal densities of light weight dynamic structures using this conductance. The conductance is however mass corrected over the frequency band of interest to identify valid modal densities of the test structures.

For this purpose a steel plate and a cylindrical shell made of a fiber composite material have been used for the experimental implementation and investigations. The modal density parameters of the steel plate have been determined using an experimental procedure and suitable measurements. Next, the modal density has been calculated for the same plate using the statistical energy analysis code AutoSEA (1999), a software tool for noise and vibration modelling, as well as simulations using the exact solution of the simply supported rectangular plate. Results obtained by the different methods have been compared graphically to show the validity of the experimental method over the theoretical methods.

The cylindrical shell has been experimentally investigated to determine the modal density parameters over a particular frequency band of interest. The same parameters have also been calculated for the purpose of comparison over the same frequency bands using AutoSEA2. The results obtained by the above mentioned methods are illustrated graphically to show the validity of each method.

2   Basic Concepts of SEA Methods

The techniques of SEA require that a complex structure is divided into a number of subsystems in order to analyse the energy distribution and energy flow between the coupled subsystems. A subsystem is considered as a group of modes which are similar in energetic terms. Next, the physical coupling between the subsystems is defined properly. Finally, the type of external excitation or input power to each subsystem is also defined. In addition to that, the power, which is dissipated internally in a subsystem, is assumed to be proportional to the energy of the subsystem.

2.1   Energy Equations for SEA Methods

Based on the above mentioned concepts, it can be stated that the net energy flow from substructure 1 to substructure 2 varies proportionally to the difference in modal energy, i.e. energy per mode in a given frequency band, and can be written using the fundamental relation of SEA (Lyon and Maidanik, 1962) as

$$\langle P_{12} \rangle \quad \propto \quad \omega \left(\frac{\langle E_1 \rangle}{N_1} - \frac{\langle E_2 \rangle}{N_2} \right) \tag{1}$$

where $\langle E_1 \rangle$ and $\langle E_2 \rangle$ are the averaged total energies of the subsystems 1 and 2, respectively, N_1 and N_2 are the number of total modes of the subsystems 1 and 2 in the frequency band $\Delta\omega$, respectively, and ω is the centre frequency of the band.
The relation in equation (1) can be rewritten as

$$\langle P_{12} \rangle = \omega \, \eta_{12} \, \langle E_1 \rangle - \omega \, \eta_{12} \frac{N_1}{N_2} \, \langle E_2 \rangle \equiv \omega \, \eta_{12} \, \langle E_1 \rangle - \omega \, \eta_{21} \, \langle E_2 \rangle \tag{2}$$

with the reciprocity equation

$$\eta_{21} = \eta_{12} \frac{N_1}{N_2} = \eta_{12} \frac{N_1/\Delta\omega}{N_2/\Delta\omega} = \eta_{12} \frac{n_1}{n_2} \tag{3}$$

In the equations (2) and (3), η_{12} and η_{21} are the coupling loss factors between the subsystems, and n_1 and n_2 are the modal densities of the subsystems in the band $\Delta\omega$.
The energy loss due to the dissipation in each subsystem is directly proportional to the total dynamical energy of the subsystem and can be evaluated by

$$\langle P_{1,diss} \rangle = \omega \, \eta_{11} \, \langle E_1 \rangle \text{ or } \langle P_{2,diss} \rangle = \omega \, \eta_{22} \langle E_2 \rangle \tag{4}$$

where η_{11} and η_{22} are the damping loss factors of the subsystems, and $\langle P_{1,diss} \rangle$ and $\langle P_{2,diss} \rangle$ are the time averaged dissipated power in the subsystems.
The global SEA equation can be calculated by balancing the time averaged external power input to subsystem 1 with the power dissipated in the subsystem and the net power flow to the coupled subsystem 2, see Figure 1.
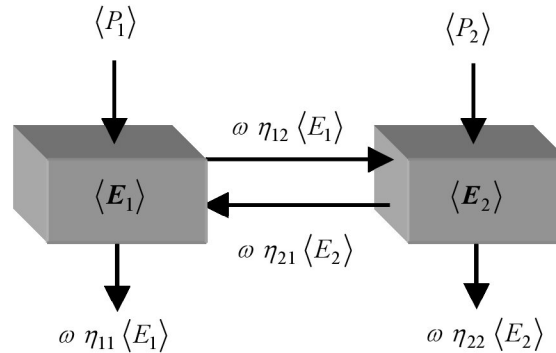
Figure 1. Basic SEA Model, Power Flow between subsystems

The balance equations of power for the two subsystems shown in Figure 1 can then be written as

$$\langle P_1 \rangle = \omega \, \eta_{11} \langle E_1 \rangle + \omega \, \eta_{12} \langle E_1 \rangle - \omega \, \eta_{21} \langle E_2 \rangle \tag{5}$$

and

$$\langle P_2 \rangle = \omega \, \eta_{22} \langle E_2 \rangle + \omega \, \eta_{21} \langle E_2 \rangle - \omega \, \eta_{12} \langle E_1 \rangle \tag{6}$$

where the coupling loss factors are, according to equation (3),

$$\eta_{21} \, n_2 = \eta_{12} \, n_1 \tag{7}$$

For N substructures the above equations can be written in matrix form (Hermann and Wyckaert, 1998)

$$
\begin{bmatrix}
\sum_{i=1}^{N} \eta_{1i} & -\eta_{21} & \cdots & -\eta_{N1} \\
-\eta_{12} & \sum_{i=1}^{N} \eta_{2i} & \cdots & -\eta_{N2} \\
\vdots & \vdots & \ddots & \vdots \\
-\eta_{1N} & -\eta_{2N} & \cdots & \sum_{i=1}^{N} \eta_{N}
\end{bmatrix}
\begin{Bmatrix}
\langle E_1 \rangle \\
\langle E_2 \rangle \\
\vdots \\
\langle E_N \rangle
\end{Bmatrix}
= \frac{1}{\omega}
\begin{Bmatrix}
\langle P_1 \rangle \\
\langle P_2 \rangle \\
\vdots \\
\langle P_N \rangle
\end{Bmatrix}
\tag{8}
$$

with

$$\eta_{ji} \, n_j = \eta_{ij} \, n_i \tag{9}$$

where η_{ii} are the internal damping loss factors of each subsystem, η_{ij} are the coupling loss factors between subsystems i and j, $\langle P_i \rangle$ the time averaged input power into subsystem i, and $\langle E_i \rangle$ the time averaged energy of subsystem i .

We can see that a realistic solution of equation (8) is only possible if the coupling loss factors fulfil the additional reciprocity equations (9). Therefore, an important condition for the SEA analysis is the knowledge of the modal densities n_i of the subsystems. For many simple structures (e.g. beams, plates, cylinders) the modal densities are known from theoretical considerations and from numerical analysis (Cremer and Heckl, 1996). However, for complicated structures or for structures with complicated material properties (orthotropic solids, foams, fibres, sandwich, composite, ribbed structures, etc.) an experimental validation of the modal densities is often needed.

2.2   Experimental Procedure for the Identification of Modal Densities of Light Weight Structures

2.2.1   Modal Density Identification

The simplest experimental method to determine the modal density is to measure some frequency response functions of the structure, to identify, and to count the number of modes in a particular frequency band. Somewhat more precise results can be achieved by the experimental modal analysis (EMA). For light weight structures (very thin sheets) these methods are only efficient for a limited frequency domain. Due to the internal damping, these methods fail in the vibro-acoustic frequency domain because of the high modal overlap. Therefore, other experimental methods are required.

A very powerful method known in the SEA is the identification of the modal density from frequency response functions measured at the driving point. This method can be described as follows:

The frequency response function, admittance $H^v(f)$ at a point (x, y) of a structure due to excitation at location (x_0, y_0) can be expressed by the following equation:

$$H^v(f) = \frac{jf}{2\pi m} \sum_r \frac{\phi_r(x,y) \, \phi_r(x_0,y_0)}{[\,(f_r^2 - f^2) + j \, \eta_r \, f_r \, f\,]} \tag{10}$$

The normalisation of the modal vectors $\phi_r(x, y)$ in equation (10) for a uniform mass density is given by

$$\frac{1}{A} \int_{(A)} \phi_k(x, y)\, \phi_l(x, y)\, dA \;=\; \delta_{k,l} \tag{11}$$

In equation (10), (x, y) are arbitrary coordinates, (x_0, y_0) are the coordinates of the excitation point, f_r is the natural frequency of the rth mode, f is the excitation frequency, η_r is the damping loss factor of the rth mode, and m is the mass of the structure.

If the admittance is measured at the driving point (x_0, y_0), then equation (10) can be rewritten as

$$H^v(f) \;=\; \frac{jf}{2\pi m} \sum_r \frac{\phi_r^2(x_0, y_0)}{[(f_r^2 - f^2) + j\eta_r f_r f]} \tag{12}$$

The real part of the admittance, i.e. the conductance, at the driving point is obtained using equation (12)

$$Re\{H^v(f)\} \;=\; \frac{1}{2\pi m} \sum_r \frac{\eta_r f_r f^2\; \phi_r^2(x_0, y_0)}{[(f_r^2 - f^2)^2 + (\eta_r f_r f)^2]} \tag{13}$$

An average value of equation (13) can be calculated over all the driving points (x_0, y_0) on the structure

$$\left\langle Re\{H^v(f)\} \right\rangle_{x_0, y_0} \;=\; \frac{1}{2\pi m} \frac{1}{A} \int_{(A)} \sum_r \frac{\eta_r f_r f^2\; \phi_r^2(x_0, y_0)}{[(f_r^2 - f^2)^2 + (\eta f_r f)^2]}\, dA \tag{14}$$

and by consideration of equation (11), the above expression may be rewritten as

$$\left\langle Re\{H^v(f)\} \right\rangle_{x_0, y_0} \;=\; \frac{1}{2\pi m} \sum_r \frac{\eta_r f_r f^2}{[(f_r^2 - f^2)^2 + (\eta f_r f)^2]} \tag{15}$$

Equation (15) describes the average conductance of a structure over all the driving points (x_0, y_0). If this average has been also taken over a frequency band Δf, then equation (15) can be reformulated as

$$\left\langle Re\{H^v(f)\} \right\rangle_{x_0, y_0, \Delta f} \;=\; \frac{1}{\Delta f} \int_{\Delta f} \frac{1}{2\pi m} \sum_r \frac{\eta_r f_r f^2}{[(f_r^2 - f^2)^2 + (\eta f_r f)^2]}\, df \tag{16}$$

Provided that the noise bandwidth $\Delta_{noise,r}$ of all the modal resonators in the frequency band Δf is

$$\Delta_{noise,r} \;\ll\; \Delta f$$

equation (16) is reduced to

$$\left\langle Re\{H^v(f)\} \right\rangle_{x_0, y_0, \Delta f} \;=\; \frac{1}{\Delta f} \frac{1}{2\pi m} \frac{\pi}{2} \sum_r 1 \;=\; \frac{1}{\Delta f} \frac{1}{4m} N_{\Delta f} \tag{17}$$

where $N_{\Delta f}$ is the number of modes in the frequency band Δf.

From equation (17) using the modal density $n(f) = N_{\Delta f}/\Delta f$ we obtain one of the most remarkable relations in the SEA (here and in the following paragraphs, f means the centre frequency of the corresponding frequency band)

$$\left\langle Re\{H^v(f)\} \right\rangle_{x_0, y_0, \Delta f} \;=\; \frac{n(f)}{4m} \tag{18}$$

This means that if the average conductance of all the driving points as well as over the frequency band Δf is known by measurements, then the modal density parameters $n(f)$ can be computed directly using the mass m of the test structure under investigation. Indeed, an essential condition is that the frequencies should lie close to each other in the frequency band.

In Figure 2 some simulation results are shown. For a simply supported flat rectangular steel plate, isotropic and homogeneous with dimensions (900 x 600 x 1.15) mm, the modal densities were calculated in 1/3 octave bands

218

from 10 Hz to 5000 Hz using equation (18). The averaged conductances were limited to only five driving points as indicated in Figure 6. The simulation results are compared to the exact values obtained by counting the number of modes and by the theoretical analysis. It can be seen that expression (18) yields fairly good results starting from 400 Hz band, and they coincide with the theoretical SEA values in the high frequency bands.
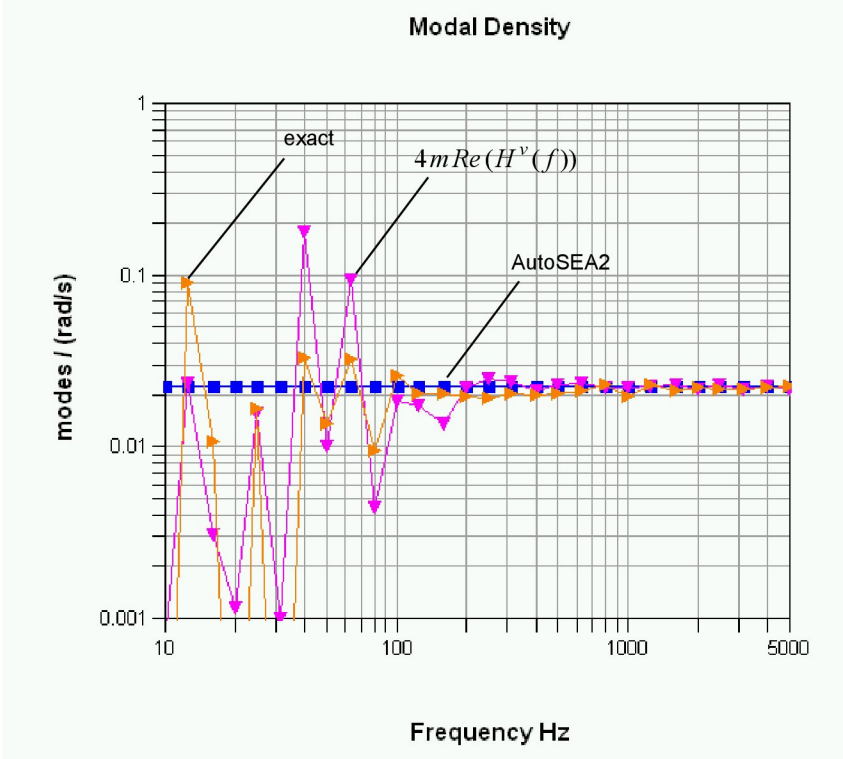
Figure 2. Comparison of AutoSEA2 and Simulation Results

In Figure 3 the modal overlap factor *MOL* of the plate is shown. This parameter gives an approximate
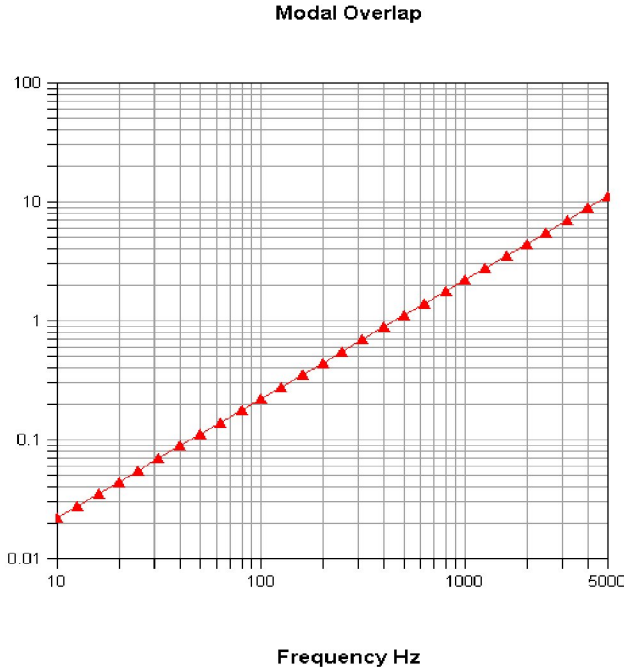
Figure 3. Modal Overlap *MOL* of the Steel Plate

219

frequency limit for the calculation of vibro-acoustic phenomena of structures and is defined as

$$MOL = n(f) \cdot \Delta_n = n(f) \cdot \frac{\pi}{2} f \eta \qquad (19)$$

where $n(f)$ is the modal density, Δ_n the noise bandwidth of the modal oscillators, f the centre frequency, and η the damping loss factor of the structure in the corresponding frequency band. For simulation purposes a loss factor $\eta = 0.01$ has been adopted. For $MOL < 1$ deterministic methods can be used, e.g. FEM and BEM. But if $MOL > 1$, then statistical methods are more qualified. From Figure 3 it is obvious that above 400 Hz, where $MOL > 1$, reliable results for the SEA are expected. These results are in accordance with the curves demonstrated in Figure 2.

2.2.2 Mass-Correction of Measured Conductance Curves

The impedance head used for the measurement of the acceleration and the excitation force is usually equipped with a small mass, called mass before force gauge. This mass and the additional piece used for fitting the impedance head to the test structure can influence the force measurement. In the lower frequency range or for compact structures, this mass Δm does not play a considerable role. Hence, its effect can be safely neglected.

For light weight structures the mass Δm can affect the measured excitation force $F(t)$ to a great extent, see Figure 4 below. It is noticed that the affected excitation force $F(t)$ does not exactly correspond to the measured force $F_M(t)$. Consequently, the real excitation force must be calculated. To find the real excitation force, the measured conductance should therefore be corrected using the analysis shown below:
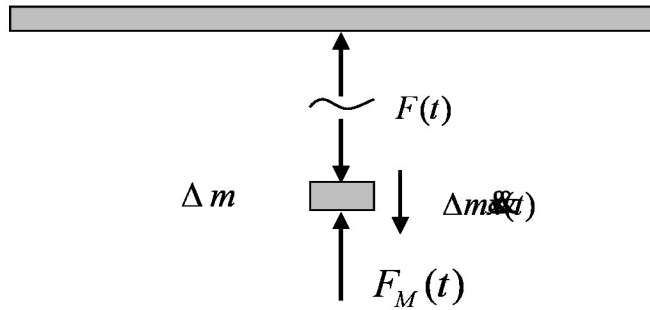
Figure 4. Mass Correction of the Excitation Force

Referring to Figure 4, the real excitation force $F(t)$ can be given by the following equation

$$F(t) = F_M(t) - \Delta m\, \ddot{a}(t) \qquad (20)$$

In the frequency domain the above equation can be written as

$$F(f) = F_M(f) - \Delta m\, a(f) \qquad (21)$$

If the acceleration $a(f)$ is replaced by the velocity $V(f)$, then this yields the following expression

$$a(f) = j\, 2\pi f V(f) \qquad (22)$$

The corrected value of the excitation force is modified to

$$F(f) = F_M(f) - j\, 2\pi f\, \Delta m\, V(f) \qquad (23)$$

and, consequently, the corrected point impedance $Z(f)$ is changed to

$$Z(f) = \frac{F(f)}{V(f)} = Z_M(f) - j\, 2\pi f\, \Delta m \qquad (24)$$

Hence the corrected real part of the admittance, i.e. the conductance, can be calculated as

$$Re\left\{H^v(f)\right\} = Re\left\{\frac{1}{Z(f)}\right\} = \frac{Re\left\{Z_M(f)\right\}}{[Re\left\{Z_M(f)\right\}]^2 + [Im\left\{Z_M(f)\right\} - 2\pi f\, \Delta m]^2}$$

In Figure 5 a measured conductance curve of the plate given in Figure 6 and the mass-corrected conductance curve calculated using the expression (25) are illustrated. The mass correction $\Delta m = 7.2$ g was measured in advance. It can be seen that the influence of the additional mass in the higher frequency bands is dominant.
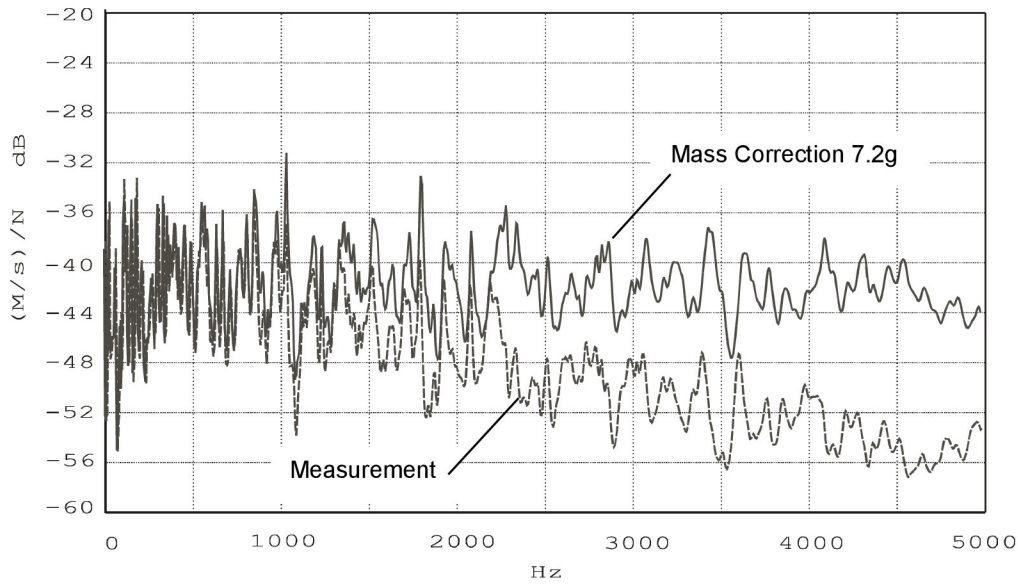
Figure 5. Mass Corrected and Actually Measured Conductances

3   Experiments and Validation of the Results

The experimental procedure outlined in section 2.2 has been applied to two light weight structures to show its effectiveness in the evaluation of the modal density parameter $n(f)$. The measurements of the excitation forces and accelerations have been carried out using a Bruel & Kjaer impedance head Type 8001 and a two channel real-time analyser Type 2144.

The experimental modal densities obtained by the above mentioned procedure have been compared with corresponding results computed by the code AutoSEA2. The experimental and theoretical analyses have been applied to two structures, i.e. a thin-walled rectangular steel plate with uniform thickness and a thin-walled cylinder made of carbon fibre reinforced plastic CFRP T800 (CFRP-cylinder), refer to Herold et al. (2001).

The details of the measurements and calculations executed for the above two examples are illustrated below.

3.1   Rectangular Steel Plate with Uniform Thickness

A rectangular steel plate has been supported horizontally and firmly fixed the four sides. It was then excited and measured as shown in Figure 6. The physical properties of the plate are: length l = 0.900 m ,width b = 0.600 m, thickness h = 0.00115 m, density ρ = 6956 kg/m³, mass m = 4.32 kg, Young's modulus E = 2.1×10^{11} N/m², shear modulus G = 8.077×10^{10} N/m², Poisson's ratio v = 0.3 .

The plate was excited at 5 different driving points with wide band noise up to 10000 Hz. The admittance at each point was measured using the impedance head. Using the experimental procedure proposed in section 2.2 and equation (18), the modal densities $n(f)$ were computed in the frequency bands from 100 Hz to 5000 Hz.

Figure 6. Steel Plate, Support, and Excitation

The experimental results are illustrated in Figure 7. We note that at a lower frequency range the experimental results are non-uniformly distributed as explained by the small modal overlap $MOL < 1$. At higher frequency bands, the modal density decreases as the frequency increases. This continuous decrease in the modal density is due to the small mass Δm as explained above.
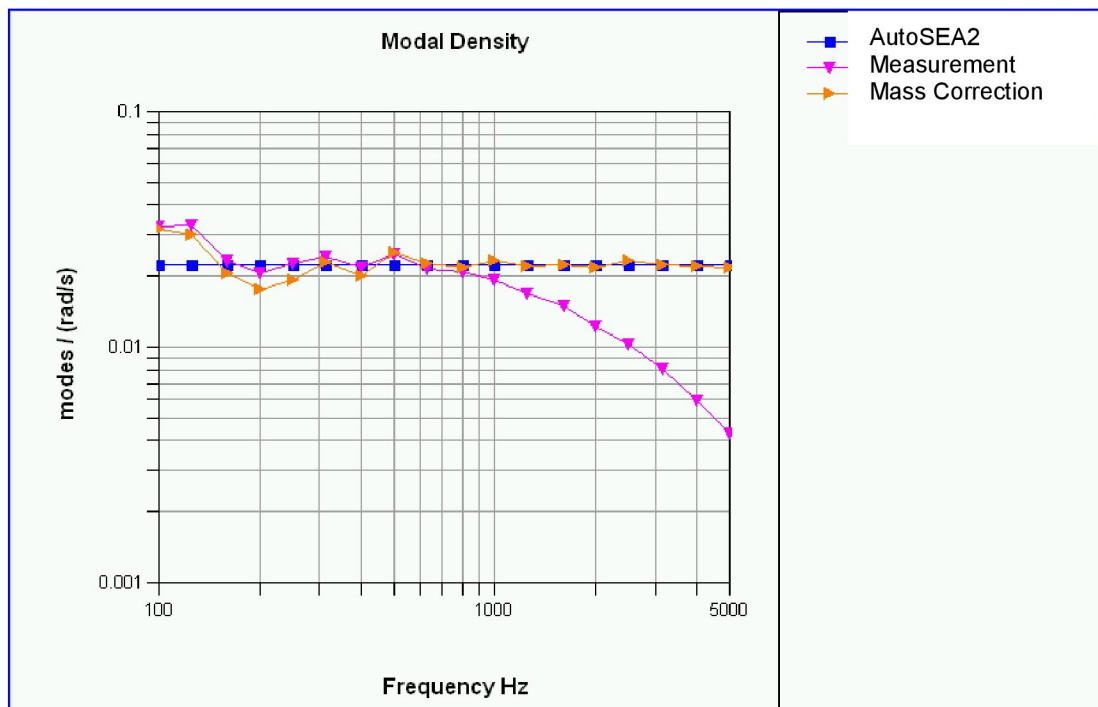
Figure 7. Results of Measurements and Calculations Using AutoSEA2

An average value of the measured modal densities at 5 driving points has been plotted without and with mass correction using equation (25). Results of modal densities obtained after the mass correction are in fairly good agreement with the theoretical results obtained by using the code AutoSEA2.

Thus, it can be concluded that the experimental modal density values over the frequency band of interest are good in high frequency ranges, and they are fluctuating in the lower frequency bands, because equation (18) is valid only for medium and high frequency bands with $MOL > 1$. However, most of the vibro-acoustical

problems occur in fact in high frequency bands and hence the values of the modal densities in higher bands are of more interest and importance than those at the lower bands.

It is clear from the results of Figure 7 that the experimental investigations using the procedure in section 2.2 can be safely applied to any light weight structure to identify the requested modal density parameter. In this way it is possible to validate the coupling loss factors given in the reciprocity equations (9).

3.2   CFRP-Cylinder

The CFRP-cylinder has been experimentally investigated to identify the modal density parameter. The test structure was soft suspended and excited as shown in Figure 8.

The material CFRP T 800 of the cylinder shell has 8 layers, each layer is 250 μm thick and quasi-isotropic with the following stacking sequence: 90,+45,0,-45,0,+45,90. The fibre content is 55-60% with hardener of type LY556-HY917. Using the above layer arrangement, the following general physical properties have been determined, $E_1 = 9.0 \times 10^{10}$ N/m², $E_2 = 2.4 \times 10^{10}$ N/m², $G = 157 \times 10^{10}$ N/m², density $\rho = 1600$ kg/m³, Poisson's ratio $\mu = 0.4$, length $L = 1.6$ m, diameter $d = 1.0$ m, average wall thickness = 0.00188 m. We note that Young's moduli in bending and shear have been validated by experiments.

Figure 8. CFRP-Cylinder with Coupled Exciter

3.2.1   Identification of Modal Density Using AutoSEA2

The code AutoSEA2 has been used to calculate the theoretical modal density $n(f)$ of the above CFRP-cylinder in the frequency bands from 100 Hz to 5000 Hz. It has been assumed here that the composite material of the CFRP-cylinder is homogeneous and orthotropic. Results obtained by AutoSAE2 are indicated in Figure 9.

3.2.2   Experimental Procedure

In order to enhance the results of the theoretical investigations experimentally, the procedure outlined in Section 2.2 has also been implemented for this case.

The cylinder was hanged vertically at two points and excited as shown in Figure 8, with wide band noise up to 10000 Hz. The experimental procedure has been applied afterwards to identify the modal densities over the frequency bands of interest. The conductance has also been mass corrected as explained in section 2.3. Results obtained by experimentation are illustrated graphically in Figure 9.

The results of the modal density parameters using the experimental procedure and the code AutoSEA2 are fairly good at the high frequency bands, as it was the case in the previous example of the steel plate, see Figure 9 for reference.

The modal overlap of the CFRP-cylinder has also been calculated with the code AutoSEA2, for which the required damping loss factors in the interested frequency bands (see equation (19)) were measured in advance. The results are shown in Figure 10. In this case the parameter *MOL* is less than unity at about 125 Hz band. Beyond this band the modal overlap is greater than unity and therefore the calculated modal density parameters are fairly identical to the experimental results as shown in Figure 9 below.
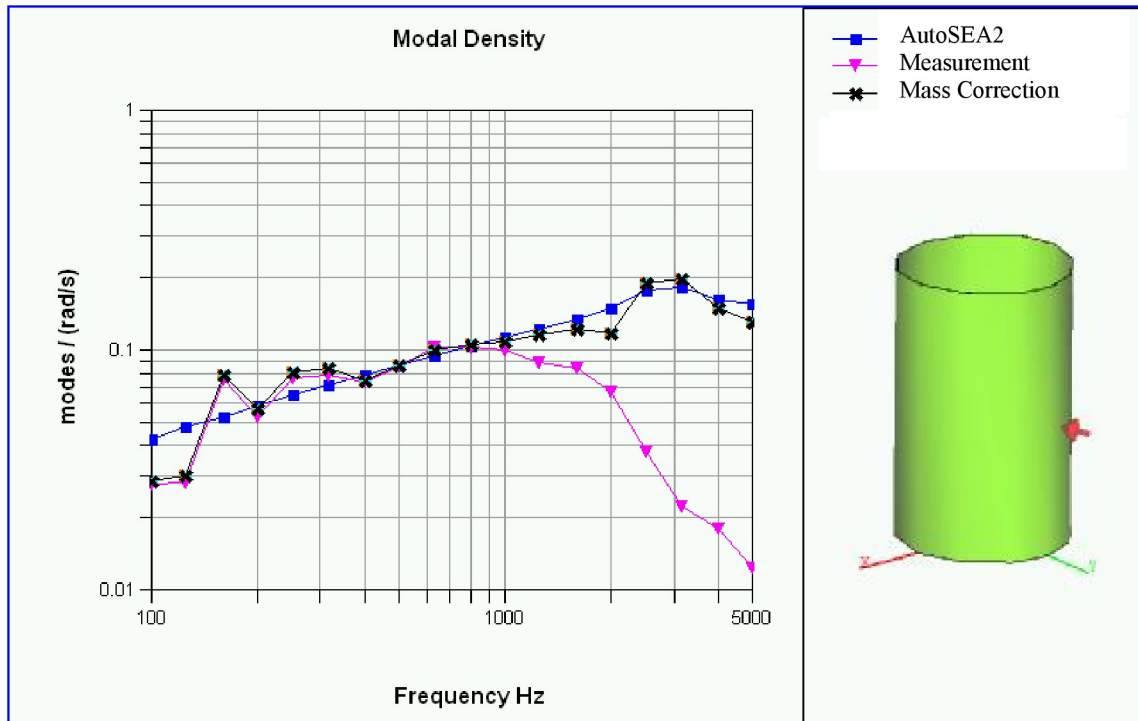
Figure 9. Measured and Theoretical Modal Densities of the CFRP-cylinder
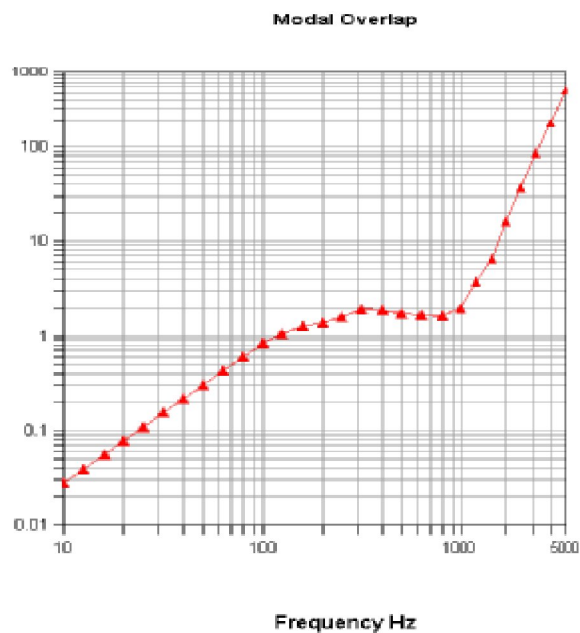
Figure 10. Modal Overlap of the CFRP-cylinder

224

4 Conclusions and Recommendation

The correct identification of the modal density parameters of a structure is very important for the statistical energy analysis SEA that is applied for the solution of vibro-acoustical problems. The modal density parameters are used to validate the reciprocity equation (3), or, in other words, the general equation (9).

It can be concluded that the statistical energy method SEA and the experimental procedure provide good results of the modal density at high frequency bands. At lower frequency bands, particularly in frequency bands with small modal overlap (MOL), i.e. when $MOL < 1$, SEA yields unsatisfactory results.

The experimental procedure has been proved to be a good tool to identify modal densities over higher frequency bands. Thus, this technique can be recommended for the identification of modal densities of light weight structures and even complex structures, because vibro-acoustical problems are always of interest at higher frequency bands.

Acknowledgement

Literature

1. Cremer L.; Heckl, M.: Körperschall, Physikalische Grundlagen und Technische Anwendungen. 2. Auflage, Springer-Verlag, (1996).
2. Herold, S; Gröbel, K. H.; Hanselka, H.; Markworth, D.; Schmidt, G.; Vogl, B.: Ein Adaptiver CFK-Zylinder – Numerische und experimentelle Ergebnisse, Abschlusskolloquium des Innovationskollegs Adaptive Mechanische Systeme, Otto-von-Guericke-Universität Magdeburg, (2001), pp. 45-54.
3. Hermann, L.; Wyckaert, K.: The Process to Experimentally Identify the Statistical Energy Analysis Parameters of Industrial Structures: Step by Step. ISMA21 – Noise and Vibration Engineering, (1996), 171-185.
4. Lyon, R. H.; DeJong R. G.: Theory & Application of Statistical Energy Analysis. Second Edition, Butterworth-Heinemann, (1995).
5. Lyon, R. H.; Maidanik, G.: Power Flow Between Linearly Coupled Oscillations, J. Acoustic Society Am. 34, (1962), 623-639.
6. Serati, P.; Marshall, S.: Comparison of Experimental and Analytical Estimates for the Modal Density of a Ring-Stiffened Cylinder. Inter-Noise Conference, (1989), 1199-1202.
7. Vibro-acoustic Sciences, Inc. AutoSEA2, Advanced Technology for Noise & Vibration Design, User's Guide, Rev. 3, 7/01 Version 2.2, (2000).

Addresses: Dr. Abdul Mannan Fareed, University of Aden, Faculty of Engineering, Crater-Aden, P.O. Box 567, Republic of Yemen; Dr. G. Schmidt, Institute of Mechanics, University of Magdeburg, Dr. F. Wahl, Institute of Mechanics, University of Magdeburg

(25)